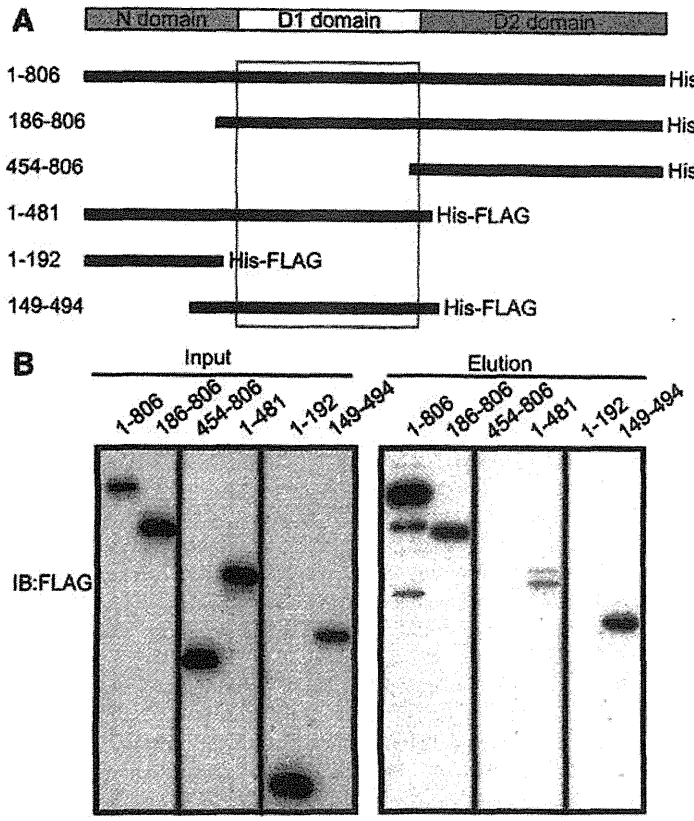

Fig. 3. Vesnarinone binds to the D1 domain of VCP. (A) Schematic structure of wild-type VCP and its derivatives used for the mutational study. VCP has an N-terminal polyubiquitin recognition domain, the D1-domain and the D2-domain. The results of the vesnarinone-binding assays are summarized to the right of the structure. (B) His-FLAG-tagged VCP deletion mutants were expressed in 293T cells and purified by using vesnarinone-immobilized beads. The input (left) and eluted (right) proteins were immunoblotted using an anti-FLAG antibody.

genes. A Western blot analysis showed that the specific siRNA reduced the level of VCP protein by >90% at 2–4 days after the siRNA transfection, whereas it had little effect on the protein level of actin (Fig. 4).

After the induction of the cells with TNFα, the expression of the NFκB target genes TNFα, IκBα, and A20 was examined by quantitative PCR. When the VCP expression was knocked down by the VCP-specific siRNA, the induction of TNFα gene expression was significantly attenuated (Fig. 4B), comparable to the result of the vesnarinone treatment (Fig. 1). In addition to the attenuation of TNFα, the induced expression of the other NFκB target genes IκBα and A20 mRNA was also attenuated (Fig. 4, C and D). These results suggest that both vesnarinone and VCP knockdown attenuate the expression of NFκB target genes in TNFα-stimulated cells by affecting NFκB activity.

This result, combined with the finding that phosphorylated IκBα is not degraded in the presence of vesnarinone (Fig. 1D), prompted us to examine the effect of the proteasome inhibitor MG132, which is known to inhibit the activation of NFκB (Hellerbrand et al., 1998). When the cells were treated with MG132, the activation levels of TNFα, IκBα, and A20 mRNA induced by TNFα were attenuated (Fig. 4) to the same level produced by the treatment with VCP siRNA. These results showed that the common effect of vesnarinone treatment and VCP knockdown are consistent with MG132 treatment, suggesting that vesnarinone inhibits the function of VCP, which is involved in a related proteasome degradation process.

Vesnarinone Treatment Enhances Ubiquitinated IκBα Accumulation. Due to the result that vesnarinone attenuates TNFα expression, we hypothesized that ubiquitinated-IκBα was not degraded but rather accumulated in the presence of vesnarinone or VCP knockdown. Thus, we examined the effect of vesnarinone on the accumulation of ubiquitinated IκB protein by performing a transient transfection of a FLAG-IκBα expression vector in 293T cells. The cells were incubated with various concentrations of vesnarinone, followed by FLAG-immunoprecipitation in a highly stringent buffer to purify and concentrate the ubiquitinated IκBα, which was detected by immunoblotting using antiubiquitin or anti-IκBα antibodies.

Predictably, the high molecular weight ubiquitinated protein detected using the antiubiquitin antibodies and the high molecular weight IκBα detected using the anti-IκBα antibodies were both enhanced in a dose-dependent manner by the treatment with vesnarinone (Fig. 5A, lanes 3–6). In addition, these signals produced similar pattern to the MG132 treatment (Fig. 5A, lane 7). Thus, we concluded that ubiquitinated IκBα accumulated after the vesnarinone treatment.

As the knockdown of VCP showed similar effects to vesnarinone, we examined whether the knockdown of VCP can also cause the accumulation of polyubiquitinated IκBα. As determined by Western blotting, the knockdown of VCP induced the accumulation of ubiquitinated IκBα (Fig. 5B). These results suggest that VCP is significant for the degradation of IκBα and the activation of NFκB.

Vesnarinone Prevents the Interaction between VCP and the 26S Proteasome. Because VCP is known to bind to ubiquitinated proteins such as IκBα, cyclin E, and hypoxia-inducible factor (HIF)1α (Dai et al., 1998; Yen et al., 2000; Dai and Li, 2001; Asai et al., 2002; Alexandru et al., 2008; Cayli et al., 2009;) and contributes to their degradation, we examined whether vesnarinone inhibits the interaction of

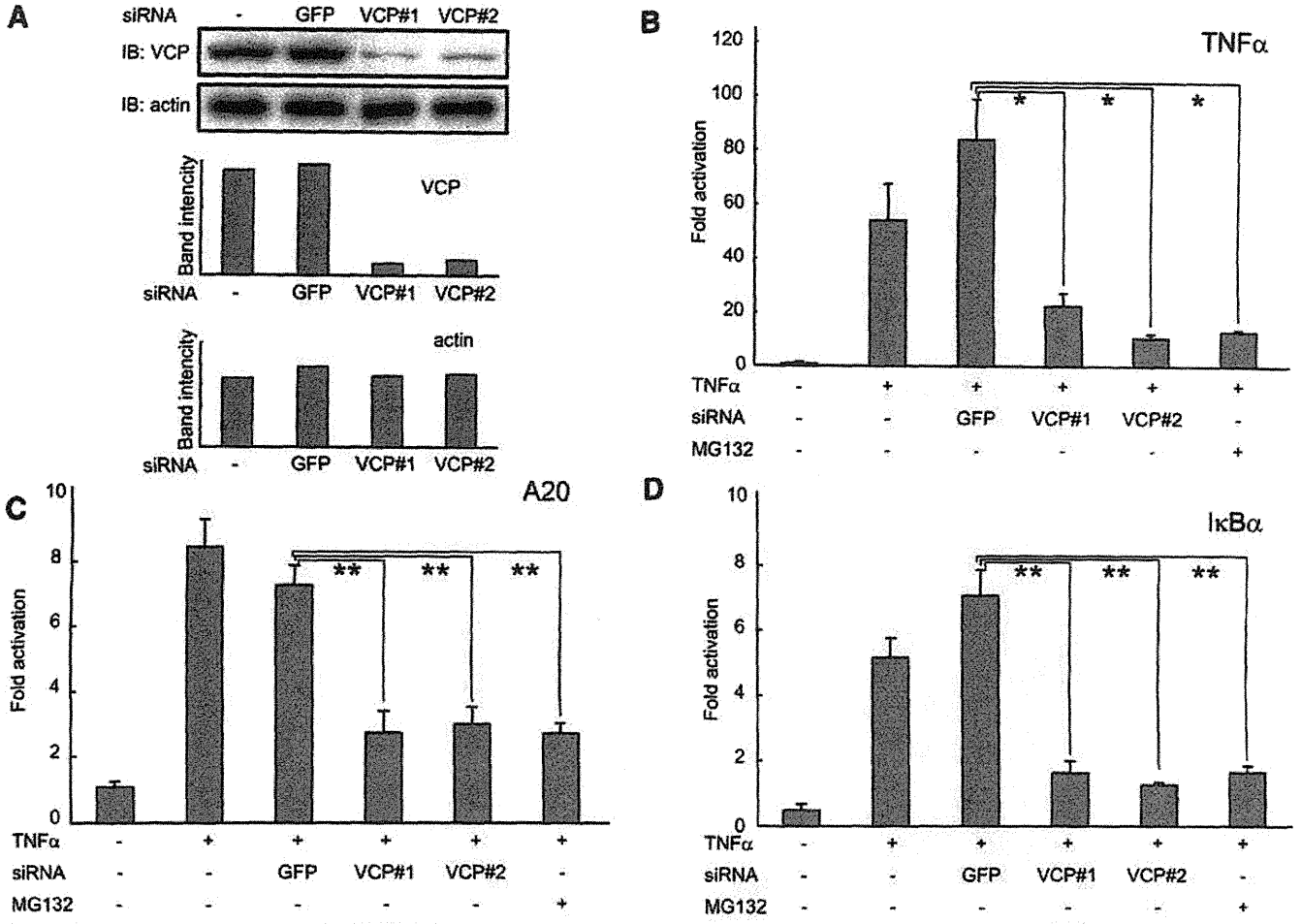

Fig. 4. VCP knockdown suppresses the TNFα-induced expression of NFκB target genes. (A) Knockdown of VCP expression by siRNA. The 293T cells transfected with the VCP- or GFP-specific siRNA were incubated for different time periods (0, 20, 25, 30, 60, 90, 120, 180 minutes from left) with 10 ng/ml TNFα, and the cell lysates were subjected to Western blot analysis using anti-VCP and anti-actin antibodies (upper panel). Lower panels show each band intensity of VCP or actin. (B–D) The 293T cells were transfected with VCP-specific siRNA or mock-transfected; 72 hours later, the cells were treated with or without TNFα for 30 minutes. The total RNA was prepared and analyzed by reverse transcription Q-PCR using primers specific for the indicated mRNAs. The data represent the average ± S.D. of three independent experiments (*$P < 0.05$; **$P < 0.01$).

VCP with ubiquitinated IκBα or the 26S proteasome. An expression vector encoding VCP-His-FLAG was transfected into 293T cells, and a coimmunoprecipitation assay was performed using an anti-FLAG antibody in the presence of MG132. As shown in Fig. 6A, in the presence of MG132, 20S C2, which is a component of the 26S proteasome, was coimmunoprecipitated with VCP-His-FLAG (Fig. 6A, lane 4), whereas 20S C2 was not precipitated without MG132 (Fig. 6A, lane 3). Interestingly, the quantity of the coprecipitated 20S C2 was reduced by increasing the amount of vesnarinone. These results suggested that vesnarinone inhibits the interaction between FLAG-tagged VCP and proteasomal 20S C2 (Fig. 6A, lanes 5–7).

When FLAG-IκBα-expressing cells were used for the coimmunoprecipitation assay, both VCP and 20S C2 were coprecipitated. In the presence of vesnarinone, the quantity of 20S C2 was reduced in a dose-dependent manner, whereas the quantity of VCP was unchanged. As the total amount of ubiquitinated IκB in the assay was almost the same, it can be concluded that vesnarinone inhibited the interaction between VCP and the 26S proteasome but not the interaction between VCP and ubiquitinated IκB.

Although we had tried to analyze the interaction between VCP and endogenous 20S C2 by coimmunoprecipitation using anti-20S C2 antibody, we failed to detect VCP or IκB with 20S C2, probably because endogenous proteosomal proteins expression was so abundant, and content of the VCP-interacted 20S C2 was quite limited in mammalian cells.

While coimmunoprecipitation assay is limited to show the interaction between VCP and ubiquitinated IκB, these results suggested that ubiquitinated IκB could interact with 20S C2 by mediating with VCP and that vesnarinone blocks proteasomal degradation of the ubiquitinated IκB by inhibiting the interaction between VCP and 20S C2.

Discussion

In this study, we showed that one of the molecular targets of vesnarinone is VCP (valosin-containing protein, also known as p97 and cdc48 in yeast), a member of the AAA ATPase family (Dai and Li, 2001). VCP is known to bind ubiquitinated proteins, such as IκBα, cyclin E, and hypoxia-inducible factor (HIF)1α and to contribute to the ubiquitin-dependent proteasome-mediated degradation of proteins (Dai et al.,

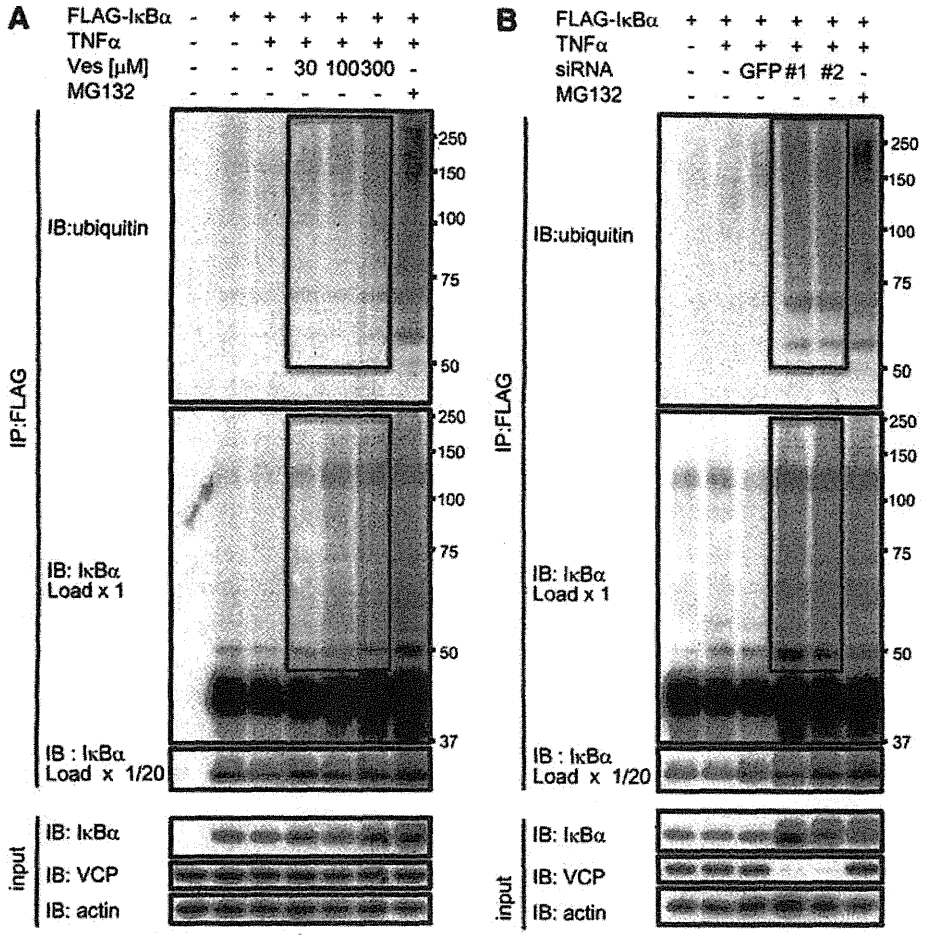

Fig. 5. Vesnarinone and VCP knockdown enhance IκBα protein accumulation. (A) Accumulation of polyubiquitinated IκB in vesnarinone-treated cells. Empty vectors (mock) or pcDNA3.1-FLAG-IκBα were transfected into 293T cells. The cells were then incubated with different concentrations (0–300 μM) of vesnarinone at 48 hours after the transfection, and the cells were treated with or without 10 ng/ml TNFα for 30 minutes at 60 hours after the transfection. The cell lysates were subjected to immunoprecipitation using an anti-FLAG antibody. The lysates (input) and immunoprecipitates were immunoblotted. (B) Accumulation of polyubiquitinated IκB in VCP knockdown cells. The cells were transfected with VCP-specific siRNA; 24 hours later, the cells were transfected with pcDNA3.1-FLAG-IκBα. After 72 hours, the cells were exposed to 10 ng/ml TNFα for 30 minutes. The cell lysates were subjected immunoprecipitation using an anti-FLAG antibody. The lysates (input) and immunoprecipitates were immunoblotted.

1998; Yen et al., 2000; Dai and Li, 2001; Asai et al., 2002; Alexandru et al., 2008; Cayli et al., 2009). Vesnarinone induced the accumulation of ubiquitinated IκBα by inhibiting the interaction between VCP and the 26S proteasome, which was essential for the degradation of IκBα and the activation of NFκB, implying that vesnarinone inhibited the function of VCP.

It has been reported that ubiquitinated IκBα remained bound to the p65-containing complexes in cells treated with a proteasome inhibitor, which also supports our results and others (Didonato et al., 1996; Roff et al., 1996). These results suggested that vesnarinone is an NFκB pathway inhibitor and that vesnarinone suppresses the activation of NFκB and the expression of TNFα mRNA by inhibiting the interaction of VCP with the 26S proteasome. As NFκB is an essential transcription factor for TNFα activation, it is reasonable that the failure of NFκB activation by vesnarinone directly affects TNFα activation. This new finding can explain our previous data and other results (Manna and Aggarwal 2000) that showed that vesnarinone inhibits the TNFα activation in HL60 and other cell lines. Although it was shown that vesnarinone inhibited the TNFα expression by inhibiting NFκB activation in a previous study (Manna and Aggarwal 2000), we could explain this inhibition based on molecular mechanisms, showing that vesnarinone inhibits the IκB degradation mediated by VCP, which is a novel molecular target of vesnarinone. One of the important differences between the present and previous study is the IκB phosphorylation status following vesnarinone treatment. While the previous study showed inhibition of IκB phosprylation by vesnarinone, we could observe IκB phosphorylation even after vesnarinone treatment. The difference may result from the difference in the cell lines, but our finding revealed another mechanism of NFκB regulation by vesnarinone.

Vesnarinone is an inotropic agent for the treatment of congestive heart failure with several known modes of action. For example, vesnarinone is known to augment sodium-calcium exchange (Yatani et al., 1989), resulting in enhanced myocardial contractility; to inhibit phosphodiesterase III (PDE3), resulting in an increase of the cyclic AMP concentration; to increase intracellular calcium ions; to alter sodium and potassium channels; and to activate the phosphorylation of cell adhesion-related molecules. Our results presented here add a new role for vesnarinone to the above list of effects.

Our study also provides new insight into the regulation of NFκB activity. As NFκB is an important transcription factor in immune responses, inflammation, cell proliferation, and other important biologic processes, it has been considered an important target for drug development. Many small molecules have been reported to be inhibitors of NFκB through their effects on the NFκB activation process.

One group of small molecule inhibitors targets the activity of NFκB. For example, gallic acid is reported to interfere with the binding activity of p65 (Choi et al., 2009). Proteasome inhibitors, such as PS-341 and PS-519, are known to inhibit

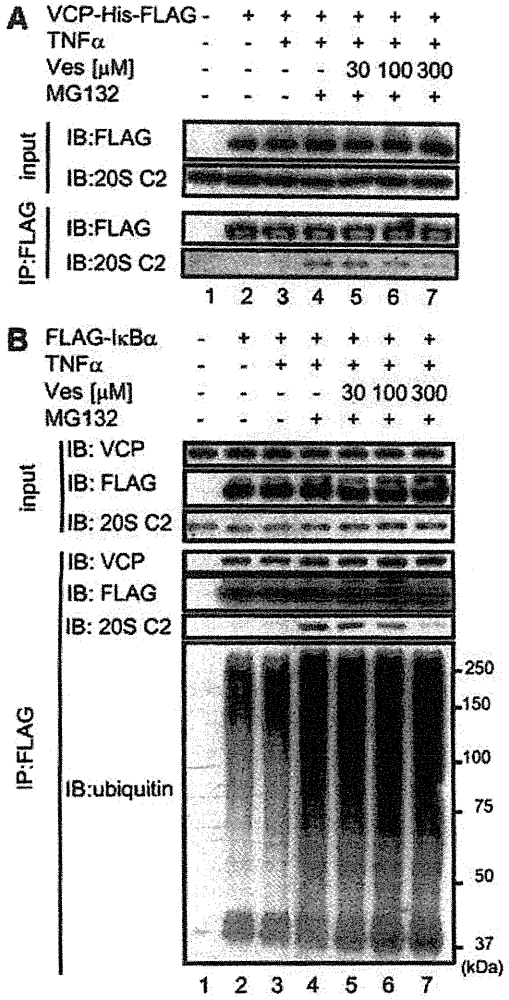

Fig. 6. Vesnarinone inhibits the interaction between VCP and the proteasome. (A) Empty vector or pHyg-EF2-VCP-His-FLAG was transfected into 293T cells; 48 hours later, the cells were treated with different concentrations (0–300 μM) of vesnarinone. Twelve hours later, the cells were treated with 5 μM MG132 for 60 minutes, followed by stimulation with 10 ng/ml TNFα for 20 minutes. The cell lysates were subjected to immunoprecipitation using an anti-FLAG antibody. The lysates (input) and coimmunoprecipitates (IP:FLAG) were immunoblotted using either anti-FLAG or anti-20S C2. (B) Either an empty vector or pcDNA3.1-FLAG-IκBα was transfected into 293T cells; 48 hours later, the cells were treated with different concentrations (0–300 μM) of vesnarinone. Twelve hours later, the cells were treated with or without 10 ng/ml TNFα for 30 minutes. The cell lysates were subjected to immunoprecipitation using an anti-FLAG antibody. The lysates (input) and coimmunoprecipitates (IP: FLAG) were immunoblotted. Co-immunoprecipitates were detected using anti-VCP, anti-FLAG, anti-20S C2, or antiubiquitin antibody.

protease activity directly (Sunwoo et al., 2001). In addition to the direct inhibition of the proteasome, the protein degradation pathway prior to proteasome entry is also a target of many compounds. For example, benzoquinones and herbimycin are known inhibitors of IκB kinase activity (Ogino et al., 2004) and sesquiterpene lactones are also hypothesized to interfere with the IκB kinase. Because vesnarinone is supposed to inhibit the interaction between VCP and a proteasome component, it can be placed in a new category, and at present no chemicals are known have the same activity. Thus, our study raises the possibility of regulating the NFκB activity by a new target molecule and VCP can be considered a novel target of antiinflammatory and immune drugs.

Recently, multiple functions of VCP have been identified (Meyer et al., 2012), including autophagy (Ju et al., 2009), endolysosomal sorting and regulation of proteins (Ritz et al., 2011), mitochondrial membrane protein turnover (Braun et al., 2006), and genome stability (Meerang et al., 2011). Although we only suggested the inhibition of the interaction between VCP and the 26S proteasome by vesnarinone in terms of NFκB inactivation, vesnarinone might affect many other biologic processes within other cellular contexts. Indeed, the examination of the function of vesnarinone via VCP within the context of different cells is an intriguing avenue of study. For example, as a previous study suggests that VCP is required for the degradation of cyclin E, a cell cycle regulator (Dai and Li, 2001), vesnarinone may influence the proliferation of cancer cells by regulating the degradation of cyclin E. In fact, vesnarinone inhibits the growth of several cancer cell lines (Honma et al., 1999; Yokozaki et al., 1999), raising the possibility that vesnarinone might have antitumor activity by affecting the function of VCP and the degradation of cyclin E. As VCP is known to have multiple functions, the refined regulation of VCP may be useful in the development of drugs that will be used for aspects other than NFκB-related processes.

In this study, we used a high-performance affinity chromatography protocol developed in our laboratory (Shimizu et al., 2000) and identified VCP as a vesnarinone-binding protein. We have previously shown that several drug targets, including thalidomide, can be identified efficiently (Ito et al., 2010) by using this technique. The identification of VCP as a molecular target of vesnarinone might have been difficult without this technique.

Authorship Contributions

Participated in research design: Kabe, Aizawa, Imai, Yamaguchi, Handa.

Conducted experiments: Hotta, Nashimoto, Yasumura, Suzuki, Azuma, Iizumi, Shima, Nabeshima, Hiramoto, Okada, Sakata-Sogawa, Tokunaga, Ando, Sakamoto.

Wrote or contributed to the writing of the manuscript: Hotta, Ito, Watanabe, Handa.

References

Alexandru G, Graumann J, Smith GT, Kolawa NJ, Fang R, and Deshaies RJ (2008) UBXD7 binds multiple ubiquitin ligases and implicates p97 in HIF1alpha turnover. *Cell* **134**:804–816.

Asai T, Tomita Y, Nakatsuka S, Hoshida Y, Myoui A, Yoshikawa H, and Aozasa K (2002) VCP (p97) regulates NFkappaB signaling pathway, which is important for metastasis of osteosarcoma cell line. *Jpn J Cancer Res* **93**:296–304.

Braun RJ, Zischka H, Madeo F, Eisenberg T, Wissing S, Büttner S, Engelhardt SM, Büringer D, and Ueffing M (2006) Crucial mitochondrial impairment upon CDC48 mutation in apoptotic yeast. *J Biol Chem* **281**:25757–25767.

Cavusoglu E, Frishman WH, and Klapholz M (1995) Vesnarinone: a new inotropic agent for treating congestive heart failure. *J Card Fail* **1**:249–257.

Cayli S, Klug J, Chapiro J, Fröhlich S, Krasteva G, Orel L, and Meinhardt A (2009) COP9 signalosome interacts ATP-dependently with p97/valosin-containing protein (VCP) and controls the ubiquitination status of proteins bound to p97/VCP. *J Biol Chem* **284**:34944–34953.

Choi K-C, Lee Y-H, Jung MG, Kwon SH, Kim M-J, Jun WJ, Lee J, Lee JM, and Yoon H-G (2009) Gallic acid suppresses lipopolysaccharide-induced nuclear factor-kappaB signaling by preventing RelA acetylation in A549 lung cancer cells. *Mol Cancer Res* **7**:2011–2021.

Cohn JN, Goldstein SO, Greenberg BH, Lorell BH, Bourge RC, Jaski BE, Gottlieb SO, McGrew 3rd F, DeMets DL, and White BG; Vesnarinone Trial Investigators (1998) A dose-dependent increase in mortality with vesnarinone among patients with severe heart failure. *N Engl J Med* **339**:1810–1816.

Dai RM, Chen E, Longo DL, Gorbea CM, and Li CC (1998) Involvement of valosin-containing protein, an ATPase Co-purified with IkappaBalpha and 26 S proteasome, in ubiquitin-proteasome-mediated degradation of IkappaBalpha. *J Biol Chem* **273**:3562–3573.

Dai RM and Li CC (2001) Valosin-containing protein is a multi-ubiquitin chain-targeting factor required in ubiquitin-proteasome degradation. *Nat Cell Biol* **3**: 740–744.

DiDonato J, Mercurio F, Rosette C, Wu-Li J, Suyang H, Ghosh S, and Karin M (1996) Mapping of the inducible IkappaB phosphorylation sites that signal its ubiquitination and degradation. *Mol Cell Biol* **16**:1295–1304.

Dignam JD, Lebovitz RM, and Roeder RG (1983) Accurate transcription initiation by RNA polymerase II in a soluble extract from isolated mammalian nuclei. *Nucleic Acids Res* **11**:1475–1489.

Fujiwara H, Arima N, Otsubo H, Matsushita K, Hidaka S, Arimura K, Kukita T, Yamaguchi K, and Tanaka H (1997) Vesnarinone exhibits antitumor effect against myeloid leukemia cells via apoptosis. *Exp Hematol* **25**:1180–1186.

Hellerbrand C, Jobin C, Iimuro Y, Licato L, Sartor RB, and Brenner DA (1998) Inhibition of NFkappaB in activated rat hepatic stellate cells by proteasome inhibitors and an IkappaB super-repressor. *Hepatology* **27**:1285–1295.

Hiramoto M, Kawakami Y, Nabeshima R, Shima D, Handa H, and Aizawa S (2004) Identification of differentiation-inducing activity produced by human bone marrow stromal cell line LP101. *Int J Mol Med* **14**:867–872.

Honma Y, Yamamoto-Yamaguchi Y, and Kanatani Y (1999) Vesnarinone and glucocorticoids cooperatively induce G1 arrest and have an anti-tumour effect on human non-small cell lung carcinoma cells grown in nude mice. *Br J Cancer* **80**:96–103.

Ito T, Ando H, Suzuki T, Ogura T, Hotta K, Imamura Y, Yamaguchi Y, and Handa H (2010) Identification of a primary target of thalidomide teratogenicity. *Science* **327**:1345–1350.

Itoh H, Kusagawa M, Shimomura A, Suga T, Ito M, Konishi T, and Nakano T (1993) Ca2+(-)dependent and Ca2+(-)independent vasorelaxation induced by cardiotonic phosphodiesterase inhibitors. *Eur J Pharmacol* **240**:57–66.

Ju J-S, Fuentealba RA, Miller SE, Jackson E, Piwnica-Worms D, Baloh RH, and Weihl CC (2009) Valosin-containing protein (VCP) is required for autophagy and is disrupted in VCP disease. *J Cell Biol* **187**:875–888.

Kubo K, Matsuzaki Y, Kato A, Terai S, and Okita K (1999) Antitumor effect of vesnarinone on human hepatocellular carcinoma cell lines. *Int J Oncol* **14**:41–46.

Manna SK and Aggarwal BB (2000) Vesnarinone suppresses TNF-induced activation of NF-kappa B, c-Jun kinase, and apoptosis. *J Immunol* **164**:5815–5825.

Matsui S, Matsumori A, Matoba Y, Uchida A, and Sasayama S (1994) Treatment of virus-induced myocardial injury with a novel immunomodulating agent, vesnarinone. Suppression of natural killer cell activity and tumor necrosis factor-alpha production. *J Clin Invest* **94**:1212–1217.

Meerang M, Ritz D, Paliwal S, Garajova Z, Bosshard M, Mailand N, Janscak P, Hübscher U, Meyer H, and Ramadan K (2011) The ubiquitin-selective segregase VCP/p97 orchestrates the response to DNA double-strand breaks. *Nat Cell Biol* **13**:1376–1382.

Meyer H, Bug M, and Bremer S (2012) Emerging functions of the VCP/p97 AAA-ATPase in the ubiquitin system. *Nat Cell Biol* **14**:117–123.

Nabeshima R, Aizawa S, Nakano M, Toyama K, Sugimoto K, Kaidow A, Imai T, and Handa H (1997) Effects of vesnarinone on the bone marrow stromal cell-dependent proliferation and differentiation of HL60 cells in vitro. *Exp Hematol* **25**:509–515.

Nio Y, Ohmori H, Minari Y, Hirahara N, Sasaki S, Takamura M, and Tamura K (1997) A quinolinone derivative, vesnarinone (OPC-8212), significantly inhibits the in vitro and in vivo growth of human pancreatic cancer cell lines. *Anticancer Drugs* **8**:686–695.

Nishio K, Masaike Y, Ikeda M, Narimatsu H, Gokon N, Tsubouchi S, Hatakeyama M, Sakamoto S, Hanyu N, Sandhu A et al. (2008) Development of novel magnetic nano-carriers for high-performance affinity purification. *Colloids Surf B Biointerfaces* **64**:162–169.

Nishizawa M, Fu S-L, Kataoka K, and Vogt PK (2003) Artificial oncoproteins: modified versions of the yeast bZip protein GCN4 induce cellular transformation. *Oncogene* **22**:7931–7941.

Ogino S, Tsuruma K, Uehara T, and Nomura Y (2004) Herbimycin A abrogates nuclear factor-kappaB activation by interacting preferentially with the IkappaB kinase beta subunit. *Mol Pharmacol* **65**:1344–1351.

Ritz D, Vuk M, Kirchner P, Bug M, Schütz S, Hayer A, Bremer S, Lusk C, Baloh RH, Lee H et al. (2011) Endolysosomal sorting of ubiquitylated caveolin-1 is regulated by VCP and UBXD1 and impaired by VCP disease mutations. *Nat Cell Biol* **13**:1116–1123.

Roff M, Thompson J, Rodriguez MS, Jacque JM, Baleux F, Arenzana-Seisdedos F, and Hay RT (1996) Role of IkappaBalpha ubiquitination in signal-induced activation of NFkappaB in vivo. *J Biol Chem* **271**:7844–7850.

Sato Y, Matsumori A, and Sasayama S (1995) Inotropic agent vesnarinone inhibits cytokine production and E-selectin expression in human umbilical vein endothelial cells. *J Mol Cell Cardiol* **27**:2265–2273.

Shimizu N, Sugimoto K, Tang J, Nishi T, Sato I, Hiramoto M, Aizawa S, Hatakeyama M, Ohba R, Hatori H et al. (2000) High-performance affinity beads for identifying drug receptors. *Nat Biotechnol* **18**:877–881.

Sunwoo JB, Chen Z, Dong G, Yeh N, Crowl Bancroft C, Sausville E, Adams J, Elliott P, and Van Waes C (2001) Novel proteasome inhibitor PS-341 inhibits activation of nuclear factor-kappa B, cell survival, tumor growth, and angiogenesis in squamous cell carcinoma. *Clin Cancer Res* **7**:1419–1428.

Yatani A, Imoto Y, Schwartz A, and Brown AM (1989) New positive inotropic agent OPC-8212 modulates single Ca^{2+} channels in ventricular myocytes of guinea pig. *J Cardiovasc Pharmacol* **13**:812–819.

Yen CH, Yang YC, Ruscetti SK, Kirken RA, Dai RM, and Li CC (2000) Involvement of the ubiquitin-proteasome pathway in the degradation of nontyrosine kinase-type cytokine receptors of IL-9, IL-2, and erythropoietin. *J Immunol* **165**:6372–6380.

Yokozaki H, Ito R, Ono S, Hayashi K, and Tahara E (1999) Effect of 3,4-dihydro-6-[4-(3,4-dimethoxybenzoyl)-1-piperazinyl]-2(1H)- quinolinone (vesnarinone) on the growth of gastric cancer cell lines. *Cancer Lett* **140**:121–128.

Address correspondence to: Dr. Hiroshi Handa, Graduate School of Bioscience and Biotechnology, Tokyo Institute of Technology, 4259 Nagatsuda-cho, Midori-ku, Yokohama, 226-8503, Japan. E-mail: handa.h.aa@m.titech.ac.jp

Reproductive Toxicology 33 (2012) 35–44

Contents lists available at SciVerse ScienceDirect

Reproductive Toxicology

journal homepage: www.elsevier.com/locate/reprotox

Involvement of gonadotropins in the induction of hypertrophy-hyperplasia in the interstitial tissues of ovaries in neonatally diethylstilbestrol-treated mice☆

Hanako Kakuta[a], Masami Tanaka[b], Pierre Chambon[c], Hajime Watanabe[d], Taisen Iguchi[d], Tomomi Sato[a,*]

[a] International Graduate School of Arts and Sciences, Yokohama City University, Yokohama 236-0027, Japan
[b] Department of Pharmacology, St. Marianna University School of Medicine, Kawasaki 216-8511, Japan
[c] Institut de Génétique et de Biologie Moléculaire et Cellulaire, CNRS/INSERM/ULP, Collège de France, BP163, 67404 Illkirch Cedex, France
[d] The Graduate University for Advanced Studies and Okazaki Institute for Integrative Bioscience, National Institute for Basic Biology, National Institutes of Natural Sciences, Okazaki 444-8787, Japan

ARTICLE INFO

Article history:
Received 13 May 2011
Received in revised form 2 October 2011
Accepted 24 October 2011
Available online 12 November 2011

Keywords:
Ovary
DES
Steroidogenesis
Interstitial cells

ABSTRACT

Neonatally diethylstilbestrol (DES) treatment causes hypertrophy-hyperplasia in the interstitial tissue of mouse ovaries. To understand the induction mechanism of the hypertrophy, mRNA expression involved in steroidogenesis in the ovary of neonatally DES-treated mice was examined. The expression of *StAR* and *Cyp11a1* was significantly reduced while *Cyp19* and *Sf-1* were stimulated in the ovary of neonatally DES-treated 3-month-old mice. Expression of those genes was not different between DES- and oil-treated mice after the gonadotropins treatment. *Lhb* in the pituitary of 3-month-old neonatally DES-treated mice was significantly decreased. Finally, ovaries from DES-treated mice transplanted to neonatally oil-treated hosts had developing follicles at several stages and corpora lutea, whereas grafted ovaries from neonatally oil-treated mice in 3-month-old neonatally DES-treated hosts showed lipid accumulation in the interstitial tissue. Thus, hypertrophy and accumulation of lipid droplets in interstitial cells of neonatally DES-treated mice is caused by impaired steroidogenesis due to the alterations of gonadotropins levels.

1. Introduction

Diethylstilbestrol (DES), a synthetic estrogen, had been prescribed for preventing abortion, however, women who were exposed to DES *in utero* developed vaginal clear-cell adenocarcinoma [1]. In mice, perinatal exposure to natural or synthetic estrogens, including DES, results in reproductive abnormalities such as absence of corpora lutea (CL), hypertrophy-hyperplasia of interstitial tissues, induction of polyovular follicles in the ovary and persistent vaginal cornification [2–6].

Hypertrophy-hyperplasia of interstitial tissues is already found in the ovary of 3-month-old prenatally DES-exposed mice, and a dramatic increase in lipid droplets in the interstitial tissue as determined by Oil Red O stain [3]. In a study of estrogen receptor α knockout (αERKO) mice, it was shown that the induction of hypertrophy-hyperplasia of interstitial tissues was mediated by ERα [7]. The absence of CL in the ovary of neonatally DES-treated mice is caused by lack of a luteinizing hormone (LH) surge [8–10]. In addition, plasma levels of testosterone (T) in neonatally DES-treated mice are lower than those in the controls, and ovariectomy, adrenalectomy or a combination of both surgeries shows no effect [11]. These results suggest that alterations in the hypothalamic–pituitary–gonadal (HPG) axis may affect steroidogenesis in the interstitial and theca cells of neonatally DES-treated mouse ovaries.

Several studies have shown that disruption of genes involved in steroidogenesis results in alterations of steroid levels and progressive increases in lipid deposits with age [12–14]. In theca and interstitial cells, cholesterol obtained from plasma lipoproteins is transferred by steroidogenic acute regulating (StAR) protein from the outer mitochondrial membrane to the inner membrane where cytochrome P450 side-chain cleaving enzyme (CYP11A1) is located [15,16]. CYP11A1 converts cholesterol to pregnenolone [15,16]. Ovaries from 8-week-old *Star* knockout (KO) mice retain a few scattered follicles and are largely composed of vacuolated stromal cells that stain with Oil Red O [12,13]. In addition, ovaries of *Cyp11a1* KO mice treated with daily injections of corticosteroids are similar to

☆ *Grant support*: This work was partially supported by a Grant-in-Aid for Scientific Research (B) (T.I.) from the Ministry of Education, Culture, Sports, Science and Technology of Japan, Grants for Strategic Research Projects at Yokohama City University (Nos. K19020, K2109, G2201 and W18005 to T.S.), a Health Sciences Research Grant from the Ministry of Health, Labor and Welfare, Japan (T.I.), and a Grant for Support of the Collaborative Study at NIBB (T.S).
* Corresponding author at: Graduate School of Nanobiosciences, Yokohama City University, 22-2 Seto, Kanazawa-ku, Yokohama 236-0027, Japan.
Tel.: +81 45 787 2394; fax: +81 45 787 2413.
E-mail address: tomomi@yokohama-cu.ac.jp (T. Sato).

0890-6238/$ – see front matter © 2011 Elsevier Inc. All rights reserved.
doi:10.1016/j.reprotox.2011.10.013

those of wild-type (WT) mice during the neonatal period, however, lipid accumulation is increased in interstitial cells around follicles at 13 days of age [14]. These results suggest that the failure of steroidogenesis leads to lipid accumulation in interstitial cells with age. Pregnenolone is converted to progesterone by 3β-hydroxysteroid dehydrogenase (3β-HSD) and/or dehydroepiandrosterone by C17-hydroxylase (CYP17A1) and then converted to androstendione by CYP17A1 and/or 3β-HSD, respectively [15,16]. Androstenedione synthesized in theca cells diffuses to granulosa cells and it is converted to T by 17β-hydroxysteroid dehydrogenase (17β-HSD) or estrone by aromatase (CYP19) and then 17β-estradiol (E2) by 17β-HSD [15,16]. Steroidogenesis is tightly regulated by the HPG axis. In theca and interstitial cells, androstenedione is produced for supplying androgen for granulosa cells to synthesize E2 in response to LH. Follicle stimulating hormone (FSH) is required for preantral to later-stage follicle development [17]. FSH also regulates the expression of CYP19 [18,19] in developing follicles where FSH receptors are located. The LH surge down-regulates this FSH-induced increase in *Cyp19* expression [20] and triggers ovulatory changes in the pre-ovulatory follicle, including luteinization of the granulosa and theca cells and production of progesterone following the expression of *Star* and *Cyp11a1* [21,22].

The orphan nuclear receptors SF-1 and LRH-1 regulate critical genes in the reproductive axis and steroidogenesis [23,24]. In the ovary, SF-1 is localized in theca, interstitial and granulosa cells [23,25,26] and activates promoters of *Star*, *Cyp11a1*, *Cyp11b1* and *Cyp21* [27,28], through the consensus T/CAAGGTCA sequence. LH reduces SF-1 expression in preovulatory granulosa cells [29]. Granulosa-specific KO mice of *Sf-1* are infertile and show hemorrhagic cysts (HC) and the absence of CL in the ovary [30] similar to the phenotype of αERKO or *Cyp19* KO mice, suggesting that *Sf-1*KO mice have the defect in the synthesis of estrogen in the ovary. LRH-1 is mainly localized in granulosa cells and CLs, and regulates *Cyp19* [23]. Mice lacking *Lrh-1* in granulosa cells are sterile due to anovulation [31]. Lack of *Lrh-1* also results in an increase of intrafollicular E2 levels with elevated *Cyp19*, and decreases of *Star* and *Cyp11a1* in granulosa cells. These results suggest that SF-1 and LRH-1 have critical roles in the ovary. Since both SF-1 and LRH-1 are expressed in granulosa cells and have similar actions [24,32], distinct differences between the actions of SF-1 and LRH-1 within the ovary are still unclear [33].

In the present study, we aimed to identify the timing of lipid droplets accumulation in interstitial cells and examined the mRNA expression involved in steroidogenesis in the ovary of neonatally DES-treated mice. We hypothesized that the altered HPG axis caused the lipid accumulation in the ovary of neonatally DES-treated mice. Therefore, ovaries from neonatally DES-treated mice were grafted under the renal capsule of ovariectomized neonatally oil-treated mice and vice versa was also examined. In addition, the serum levels of E2 in neonatally oil- and DES-treated mice were measured to assess steroidogenesis in the ovary and the expression of gonadotropin-related genes in the anterior pituitary was examined.

2. Materials and methods

2.1. Animals and treatments

C57BL/6J mice (CLEA Japan, Tokyo, Japan) were maintained on a 12-h light/12-h dark cycle (lights off at 2000 h) with controlled temperature (25 °C) and mice were given a commercial diet (MF, Oriental Yeast Co., Tokyo, Japan) and fresh tap water *ad libitum*. All animals were maintained in accordance with the NIH guide for the care and use of laboratory animals. All experiments were approved by the institutional animal care committee of the Yokohama City University. Female pups were given daily subcutaneous (s.c.) injections of 3 μg DES (Sigma Chemical Co., St. Luis, MO) dissolved in 0.02 ml sesame oil or the vehicle alone for 5 days starting on the day of birth. Female mice were killed by cervical dislocation and weighed at 1, 1.5, 2 or 3 months of age. Ovaries were weighed, fixed for histological analysis or frozen for quantitative real-time RT-PCR analysis.

Three-month-old C57 BL/6J mice treated neonatally with oil or DES were administered with 5 IU of PMSG intraperitoneally (i.p.) followed by 5 IU hCG 48 h later. Ovaries were dissected 8 h after the hCG injection and frozen for quantitative real-time RT-PCR.

αERKO mice were obtained by mating mice of a mixed C57BL6/129Sv background that were heterozygous for *Erα* disruption as described previously [34]. Female pups of wild-type (WT) and αERKO mice were given daily s.c. injections of 3 μg DES dissolved in sesame oil or vehicle alone for 5 days starting on the day of birth. Female mice were killed by cervical dislocation at 4 or 8 months of age. Ovaries were weighed and fixed for histological analysis.

2.2. Histological analysis

Left ovaries were fixed in Bouin's solution overnight, dehydrated through a graded series of ethanol, embedded in paraffin and serially sectioned at 8 μm. Sections were deparaffinized, hydrated through a graded series of ethanol and stained with hematoxylin and eosin (HE). Right ovaries were fixed in 10% formalin neutral buffer solution (Wako Pure Chemical Industries, Osaka, Japan) overnight, then immersed in 8% sucrose in phosphate buffered saline (PBS, pH 7.4). Frozen sections (6 μm thickness) were washed in purified water, rinsed with 60% isopropyl alcohol (Wako), stained with a freshly prepared Oil Red O (MERCK KGaA, Darmstadt, Germany) working solution at 37 °C for 15 min. Sections were rinsed with 60% isopropyl alcohol, washed in purified water and counterstained with hematoxylin. Four to 8 mice were examined in each group for histological analysis.

2.3. Immunohistochemistry

Left ovaries from oil- or DES-exposed mice were fixed in 4% paraformaldehyde (MERCK KGaA) in PBS at 4 °C overnight, embedded in paraffin and serially sectioned at 5 μm for CYP11A1, SF-1 and estrogen receptor β (ERβ) immunohistochemistry. Sections were mounted on silane (3-aminopropyl triethoxy-silane, Sigma)-coated glass slides, deparaffinized and hydrated through a graded series of ethanol. After washing in purified water, slides were microwaved for 5 min for SF-1 and 8 min for ERβ staining in 10 mM sodium citrate buffer (pH 6.0) for antigen retrieval. Endogenous peroxidase activity was blocked by 1% H_2O_2 in ion-exchanged water for 10 min. Then sections were washed in PBS and incubated with normal blocking serum (VECTASTAIN Elite ABC kit, Vecter Laboratories, Inc., Burlingame, CA) for CYP11A1 and ERβ staining and 5% bovine serum albumin (Sigma) in PBS for SF-1 staining for 30 min. After washing in PBS, sections were incubated with rabbit polyclonal antibody against rat CYP11A1 (1:5000 dilution, Chemicon International, Inc., Temecula, CA), rabbit polyclonal antibody against bovine SF-1 (1:10 000 dilution; a gift from Dr. Y. Ikeda, School of Mecidine, Yokohama City University), rabbit polyclonal antibody against mouse ERβ (1:250 dilution, Zymed Laboratories, San Francisco, CA), or rabbit immunoglobulin fraction (Dako Cytomation, Glostrup, Denmark) as a negative control at 4 °C overnight. For SF-1 and ERβ staining, sections were washed in PBS and incubated with biotinylated secondary antibody (Vector Laboratories) for 30 min. After washing in PBS, sections were incubated with avidin–biotin complex (ABC) reagents (Vector Laboratories) for 30 min according to the manufacturer's protocol. For CYP11A1 staining, sections were washed in PBS and incubated with histofine simple stain PO (R) (Nichirei Co., Tokyo, Japan) for 45 min. Reaction products were visualized using 1 mg/ml 3,3′-diaminobenzidine (DAB, Sigma) in PBS containing 1% H_2O_2 and sections were counterstained with hematoxylin. Five mice were examined in each group for immunohistochemical analysis.

2.4. Quantitative real-time RT-PCR

Ovaries from 1.5- and 3-month-old mice treated neonatally with oil or DES, and anterior pituitaries from 3-month-old mice treated neonatally with oil or DES were homogenized in TRIzol (Invitrogen Co., Carlsbad, CA). Total RNA isolated from ovaries and pituitaries was purified by DNase I (Roche, Penzberg, Germany) to remove genomic DNA, cleaned up with an RNeasy total RNA kit (Qiagen, Chatswoth, CA) and reverse transcribed into cDNA by SuperScript II reverse transcriptase (Invitrogen) using oligo dT primer (Invitrogen). Real-time PCR was carried out with a Smart Cycler II System (Takara Bio Inc., Otsu, Japan) with SYBR Premix Ex Taq™ (Takara). Relative mRNA expression of *Star*, *Cyp11a1*, *Cyp19*, *Hsd3b1*, *Hsd3b1*, *Hsd3b6*, *Hsd17b1*, *Hsd17b3*, *Sf-1*, *Lrh-1*, *Cga*, *Fshb*, *Lhb* and peptidylprolyl isomerase A (*Ppia*) was determined by the standard curve method. Primer sequences are indicated in Supplemental Table 1. *Ppia* was chosen as an internal standard to control for variability in amplification due to differences in starting mRNA concentration. One ovary or anterior pituitary per mouse was examined in each group and 3 (ovary) or 5 (pituitary) independent experiments were carried out for quantitative real-time RT-PCR analysis.

2.5. Radioimmunoassay

Neonatally oil- or DES-treated 1.5- and 3-month-old mice were anaesthetized with diethyl ether (Wako) and blood was collected via the ascending jugular vein into tubes. The serum was isolated by centrifugation at 3000 rpm for 15 min and stored at −80 °C before use. The serum E2 level was estimated by DPC ^{125}I radioimmunoassay kit, E2 double antibody, KE2D1 (Siemens Healthcare Diagnostics Inc., Los

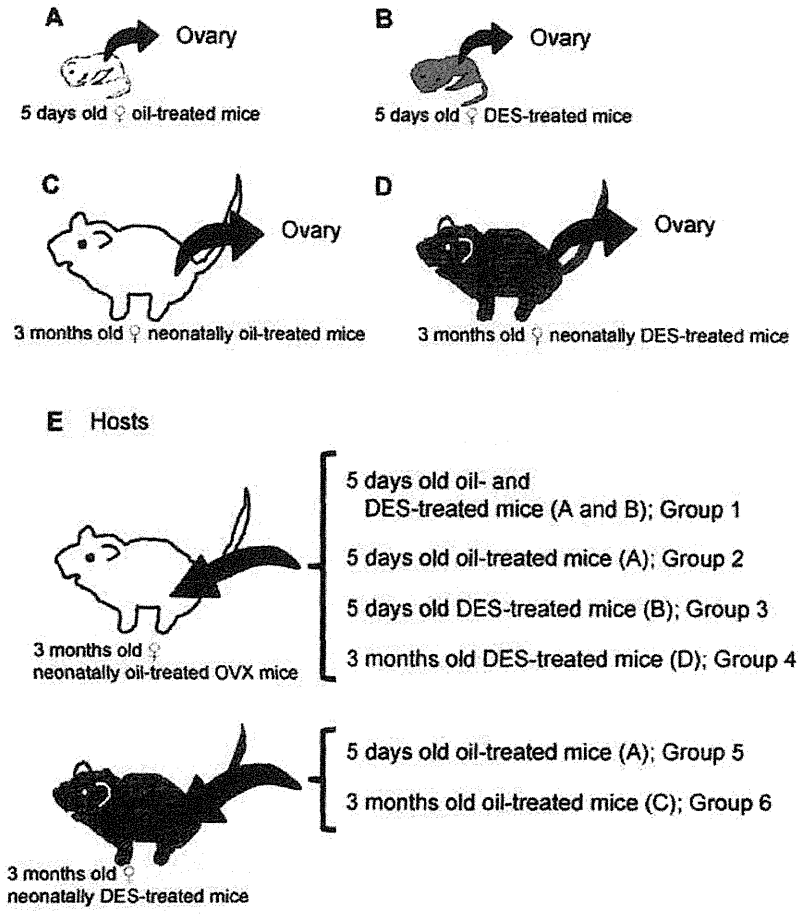

Fig. 1. Experimental design. White mice indicate neonatally oil-treated mice and black mice indicate neonatally DES-treated mice, respectively. Ovaries from 5-day-old oil- (A) or DES-treated mice (B) were transplanted under the renal capsule of the same ovariectomized adult mice (group 1), ovaries from 5-day-old oil-treated mice (A) were transplanted under the renal capsule of ovariectomized adult mice (group 2), ovaries from 5-day-old DES-treated mice (B) were transplanted under the renal capsule of ovariectomized adult mice (group 3), ovaries from 3-month-old mice treated neonatally with DES (D) were transplanted under the renal capsule ovariectomized adult mice (group 4), ovaries from 5-day-old oil-treated mice (A) were transplanted under the renal capsule of 3-month-old neonatally DES-treated adult mice (group 5), ovaries from 3-month-old oil-treated mice (C) were transplanted under the renal capsule of neonatally DES-treated 3-month-old mice (group 6), respectively. Ovx; ovariectomized mice.

Angeles, CA). The serum from each mouse was pooled up to 200 μl and 6–9 points were examined in each group for radioimmunoassay.

2.6. Tissue grafting

Six different groups of tissue grafting were shown in Fig. 1; ovaries from 5-day-old oil- or DES-treated mice were transplanted under the renal capsule of the same ovariectomized adult mice (group 1), ovaries from 5-day-old oil-treated mice were transplanted under the renal capsule of ovariectomized adult mice (group 2), ovaries from 5-day-old DES-treated mice were transplanted under the renal capsule of ovariectomized adult mice (group 3), ovaries from 3-month-old mice treated neonatally with DES were transplanted under the renal capsule ovariectomized adult mice (group 4), ovaries from 5-day-old oil-treated mice were transplanted under the renal capsule of neonatally DES-treated adult mice (group 5), and ovaries from 3-month-old oil-treated mice were transplanted under the renal capsule of neonatally DES-treated adult mice (group 6). At the end of the 3-month growth period, grafted ovaries were fixed in Bouin's solution or 10% formalin neutral buffer solution for histological analysis. Four to 9 host mice and 8–18 grafted ovaries were examined in each group for histological analysis.

2.7. Statistical analysis

Data are expressed as the mean ± standard error. For multiple comparisons, treatment groups were compared using analysis of variance (ANOVA) followed by Dunnett's post hoc test. Two-tailed Student's *t*-test was used for single comparison. Fisher's exact probability test was used to examine the significance of the association between the two kinds of classification. A statistically significant difference was defined as $p < 0.05$.

3. Results

3.1. Lipid accumulation in the ovary and involvement of ERα

Ovaries from 1-month-old neonatally oil- or DES-treated mice did not stain with Oil Red O (data not shown). CL in the ovaries of oil-treated mice were weakly stained with Oil Red O at 1.5 and 3 months of age (Fig. 2A and B). The interstitial and theca cells in the ovaries of neonatally DES-treated 1.5- and 3-month-old mice (Fig. 2A and B) stained with Oil Red O. In addition, the interstitial tissues of 3-month-old neonatally DES-treated mice showed medullary tubule-like structures. No CL was found in the ovary of 3-month-old neonatally DES-treated mice (Fig. 2A and B).

To examine the involvement of ERα in lipid accumulation, ovaries from 4- and 8-month-old neonatally oil- or DES-treated WT and αERKO mice were stained with Oil Red O. The interstitial tissue and CL in the ovaries of 4-month-old neonatally oil-treated WT mice slightly stained with Oil Red O (Fig. 2C). The interstitial regions of neonatally DES-treated WT mice showed medullary tubule-like structures. The interstitial and theca cells of neonatally DES-treated WT mice showed strong Oil Red O staining both in 4 and 8 months of age (Fig. 2D and H) and the stained area was increased in the ovaries of 8-month-old neonatally oil-treated WT mice (Fig. 2H). Ovaries from neonatally oil- or DES-treated αERKO mice showed

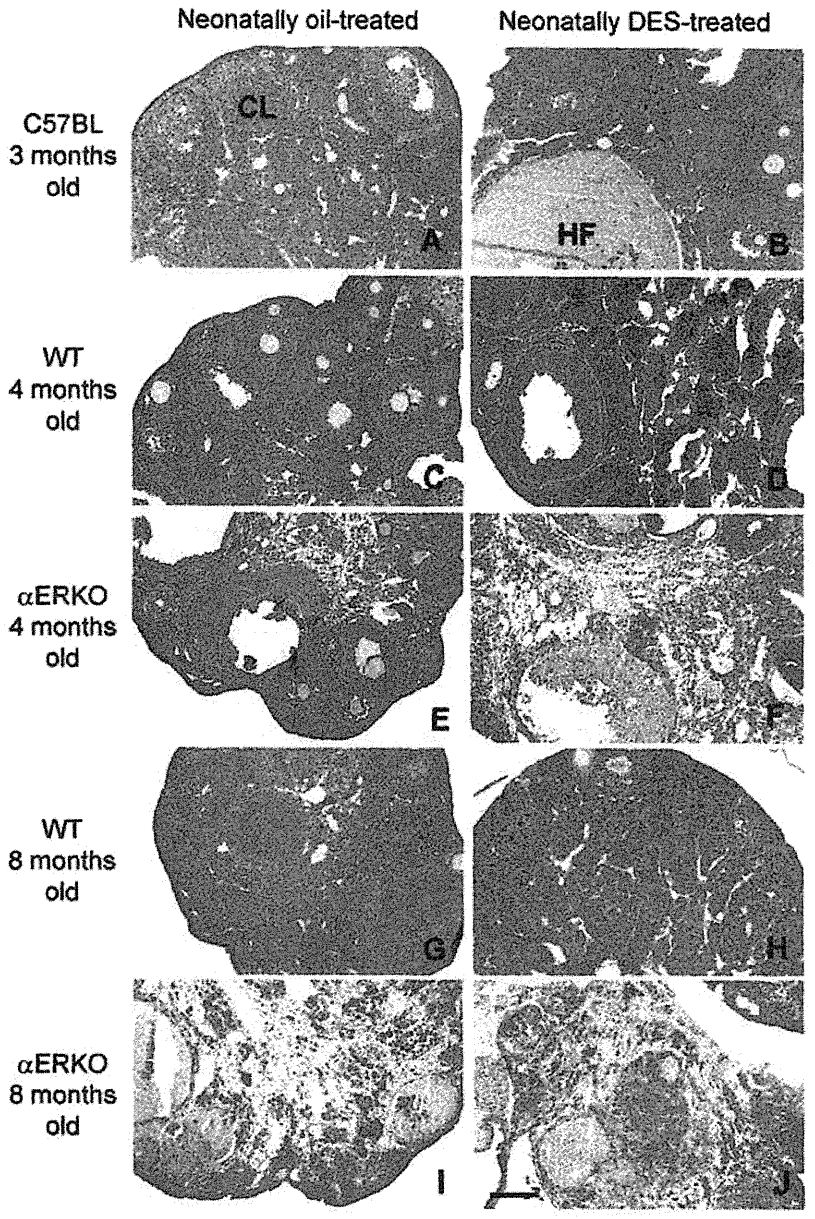

Fig. 2. Oil Red O staining in the ovary of neonatally oil- (A, C, E, G and I) or DES-treated (B, D, F, H and J) C56BL/6J (A and B), wild type (WT) (C, D, G and H) or ERα knockout (αERKO) mice (E, F, I and J), respectively. Ovaries from 3-month-old (A and B), 4-month-old (C–F) and 8-month-old (G–J) mice, respectively. CL; corpus luteum, HF; hemorrhagic follicle. Bar = 200 μm.

similar staining in the interstitial tissues with Oil Red O (Fig. 2E, F, I and J), but the stained area of the interstitial tissues was increased at 8 months of age both in the ovaries of neonatally oil- and DES treated αERKO mice (Fig. 2I and J).

3.2. Expression of genes involved in ovarian steroidogenesis

To examine the expression of genes involved in ovarian steroidogenesis in ovaries of oil- or DES-treated mice, real-time RT-PCR was performed. In 1.5-month-old neonatally DES-treated mice, the expression of *Star* was significantly decreased and the expression of *Lrh-1* was significantly increased compared with those in oil-treated mice (Fig. 3A). In 3-month-old neonatally DES-treated mice, the expression of *Star* and *Cyp11a1* was significantly decreased and the expression of *Cyp19* and *Sf-1* was significantly increased compared with those in oil-treated mice (Fig. 3A). The expression of *Hsd3b1*, *Hsd3b6*, *Hsd17b1* and *Hsd17b3* was not changed in neonatally DES-treated mice (Fig. 3B).

3.3. Localization of CYP11A1 and SF-1

CYP11A1 immunoreactivity localized in the cytoplasm of the interstitial and theca cells of both neonatally oil- and DES-treated mice at 1.5 and 3 months of age (Fig. 4A–D). The expression of CYP11A1 in the interstitial cells of 3-month-old neonatally DES-treated mice was slightly weaker than that in oil-treated mice (Fig. 4C and D). CL in the ovary of neonatally oil-treated 1.5- and 3-month-old mice also showed the expression of CYP11A1.

SF-1 immunoreactivity localized in the nuclei of the interstitial and theca cells of both 3-month-old oil- and DES-treated mice and the staining intensity was not changed in DES-treated mice (Fig. 4E and F).

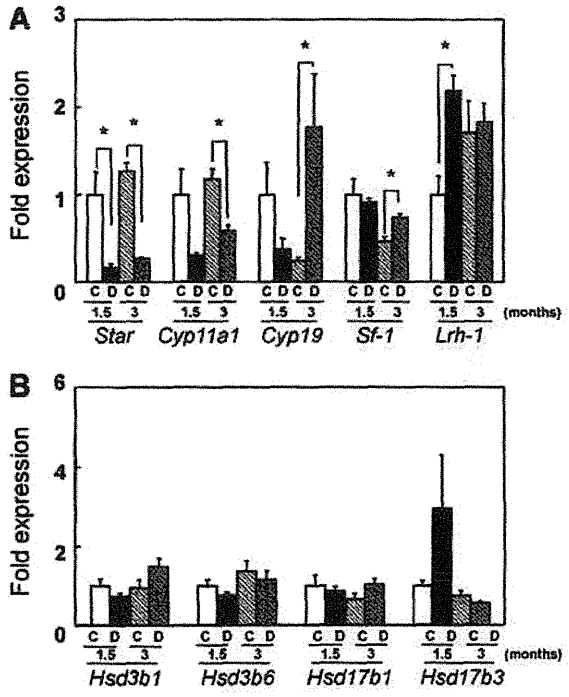

Fig. 3. Changes in the mRNA expression involved in ovarian steroidogenesis in the ovary of 1.5- and 3-month-old neonatally oil- or DES-treated C56BL/6J mice (A, B). C: neonatally oil-treated mice, D: neonatally DES-treated mice. *; $p < 0.05$, compared with age-matched oil-treated mice.

3.4. Expression of Erα and Erβ mRNAs and ERβ protein

The expression of *Erβ* mRNA in 1.5- and 3-month-old neonatally DES-treated mice was significantly increased compared with that in oil-treated mice, whereas *Erα* mRNA expression was not changed (Fig. 5B). The ERβ protein was found in the nuclei of granulosa cells both in oil- and DES-treated mice (Fig. 5C).

3.5. Effects of gonadotropin treatments on the expression of genes involved in ovarian steroidogenesis

Since genes involved in ovarian steroidogenesis are highly regulated by gonadotropins, and neonatally DES-treated mice showed reduced FSH levels [35], the effects of PMSG and hCG treatments on steroidogenesis in DES-treated mice were examined. The expression of *Star* was increased and *Cyp19*, *Sf-1* and *Erβ* expression was decreased by PMSG and hCG treatments both in 3-month-old neonatally oil- and DES-treated mice (Fig. 6A). The expression of *Cyp11a1* was increased only in 3-month-old neonatally DES-treated mice with PMSG and hCG treatments and there was similar expression in oil-treated mice.

3.6. Serum 17β-estradiol levels and expression of gonadotropin-related genes in the anterior pituitary

The serum E2 levels were not changed in neonatally DES-treated mice at 1.5 and 3 months of age compared with those in oil-treated mice (Fig. 6B). To examine the expression of genes involved in gonadotropins in pituitaries of oil- or DES-treated mice, real-time RT-PCR was performed. The expression of *Lhb* mRNA in 3-month-old neonatally DES-treated mice was

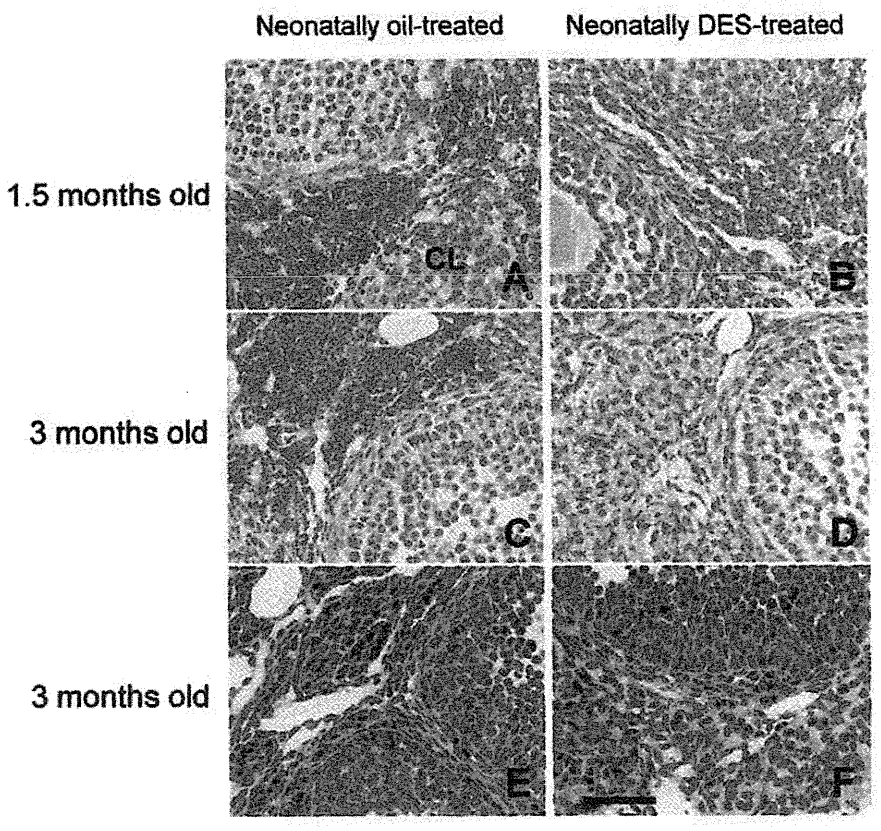

Fig. 4. Immunohistochemistry for CYP11A1 in the ovaries of 1.5-month-old neonatally oil-treated mice (A), 1.5-month-old neonatally DES-treated mice (B), 3-month-old neonatally oil control mice (C) and 3-month-old neonatally DES-treated mice (D). Immunohistochemistry for SF-1 in the ovary of 3-month-old neonatally oil-treated mice (E) and 3-month-old neonatally DES-treated mice (F). Bar = 50 μm. CL: corpus luteum.